

In Vivo Determination of Mitochondrial Respiration in 1-Methyl-4-Phenyl-1,2,3,6-Tetrahydropyridine-Treated Zebrafish Reveals the Efficacy of Melatonin in Restoring Mitochondrial Normalcy

María E. Díaz-Casado,^{1,2} Iryna Rusanova,^{1,2} Paula Aranda,^{1,2} Marisol Fernández-Ortiz,^{1,2} Ramy K.A. Sayed,^{1,3} Beatriz I Fernández-Gil,^{1,2} Agustín Hidalgo-Gutiérrez,^{1,2}
Germaine Escames,^{1,2} Luis C. López,^{1,2} and Darío Acuña-Castroviejo^{1,2,4}

¹Instituto de Biotecnología, Centro de Investigación Biomédica, Parque Tecnológico de Ciencias de la Salud, Universidad de Granada, Granada, Spain.

²Departamento de Fisiología, Facultad de Medicina, Universidad de Granada, Granada, Spain.

³Department of Anatomy and Histology, Faculty of Veterinary Medicine, Assiut University, Assiut, Egypt.

⁴Unidad de Gestión Clínica de Laboratorios Clínicos, CIBER de Fragilidad y Envejecimiento, Ibs.Granada, Complejo Hospitalario de Granada, Granada, Spain.

Abstract

Although mitochondria dysfunction is related to multiple diseases, no *in vivo* studies are available on mitochondrial respiration in animal parkinsonian models. Our aim is to analyze *in vivo* mitochondrial respiration, which reflects changes in mitochondrial bioenergetics more precisely than *in vitro* mitochondrial preparations. These experiments can be carried out in zebrafish embryos, which were treated with 1-methyl-4-phenyl-1,2,3,6-tetrahydropyridine (MPTP) from 24 to 72 hours postfertilization (hpf). A reduction in electron transfer system capacity, ATP turnover, and increased proton leak were observed at 72 hpf in MPTP-treated embryos. These changes were followed by a significant oxidative stress due to inhibition in antioxidative defense and autophagy impairment. After removing MPTP from the treatment at 72 hpf, these bioenergetic deficiencies persisted up to 120 hpf. The administration of melatonin to zebrafish embryos at 72 hpf, when mitochondrial dysfunction is already present, restored the respiratory capacity and ATP production, reduced oxidative stress, and normalized autophagy after 48 h. Melatonin also counteracted mortality and embryonic malformations due to MPTP. Our results confirm for the first time the efficacy of melatonin in restoring parkinsonian phenotypes in animals.

Keywords: *in vivo* respiration, ETS capacity, proton leak, zebrafish embryos, melatonin

Introduction

Although it is unclear whether mitochondrial dysfunction is a cause or consequence of Parkinson's disease (PD), it plays an essential role in the pathophysiology of the disease.^{1,2} Mitochondria impairment in PD not only causes a bioenergetic failure but also enhances free radicals formation, leading to a hyperoxidative condition, which ultimately triggers autophagy/mitophagy pathways and cell death.^{3,4} Impairment of mitochondrial complex I (CI) activity in the substantia nigra is typically associated with PD^{2,5} and it can be replicated under experimental conditions. The neurotoxin 1-methyl-4-phenyl-1,2,3,6-tetrahydropyridine (MPTP) is widely used to induce key features of PD, including CI inhibition, neuroinflammation, and dopaminergic cell death, in experimental animals.⁶ Melatonin, (*N*-acetyl-5-methoxytryptamine [aMT]) is a highly conserved indoleamine present in all cellular compartments, including the mitochondria,⁷ which are the principal intracellular targets of melatonin.⁸ Melatonin boosts mitochondrial activity not only by removing free radicals but also by directly stimulating the activity of the respiratory complexes and the ATP production.^{8,9}

An evaluation of mitochondrial function is critical to determine the degree of neuronal

damage in PD. Mitochondrial respiration and bioenergetic capacity have been extensively investigated in different PD models, particularly with respect to cells and small mammals.^{10,11} With regard to mammals, it is necessary to sacrifice the animal and to prepare mitochondria from substantia nigra. During this procedure, most of the damaged mitochondria are lost, with only those with relatively good membrane integrity resisting, and constituting a pool for use in respiration analysis. The bioenergetic condition of these mitochondria therefore probably tends to be overstated.¹²

To overcome these limitations, we used 72–120 hours postfertilization (hpf) zebrafish embryos to analyze mitochondrial function *in vivo*. Given that Clark electrodes are insufficiently sensitive to detect oxygen consumption changes in a living animal, we used the Seahorse Bioscience microplate-based extracellular flux analyzer, which can detect mitochondrial function *in vivo* over time and simultaneously enable the drugs required for respirometric and ATP turnover analysis to be administered.^{13,14}

We recently published a report on an experimental model of Parkinsonism in zebrafish embryos, which were used to analyze the expression of genes involved in regulating mitochondrial function.¹⁵ We found that melatonin restored the PINK1/Parkin network inhibited by MPTP and hypothesized that this enabled melatonin to revive the capacity of this network to remove damaged mitochondria in these embryos. The removal of damaged mitochondria in the brain of parkinsonian zebrafish reduced oxidative stress and neuroinflammation, thus restoring normal motor activity.¹⁵ These results suggest that parkinsonian neurodegeneration in zebrafish embryos depends on the accumulation of damaged mitochondria, which create a hyperoxidative environment.

The aim of this study is to determine whether the administration of melatonin restores mitochondrial function impaired by MPTP in a similar parkinsonian zebrafish model. As melatonin is also present in zebrafish,¹⁶ we decided that it would be useful to determine whether the neuroprotective effects of melatonin in parkinsonian zebrafish embryos, reported elsewhere,¹⁵ depend on a restoration of mitochondrial function. We also show how melatonin restores MPTP-treated embryos to mitochondrial normalcy.

Materials and Methods

Fish maintenance

AB-strain adult zebrafish (*Danio rerio*), provided by ZFBiolabs S.L (Madrid, Spain), were used as breeding stocks. The fish were kept at the University of Granada's facility at a water temperature of 28.5 – 1°C during photoperiod of 14:10 h (lights on at 08:00 h) in a recirculation aquaculture system (Aquaneering Incorporated, Barcelona, Spain). Embryos were obtained from mating pairs of adult zebrafish and were cultured in E3 medium. Fish feeding, breeding, and maintenance were performed according to the published protocols.¹⁷

All experiments were performed according to a protocol approved by the Institutional Animal Care and Use Committee of the University of Granada (procedures CEEA 2009-254 and 2010-275) and in accordance with the European Convention for the Protection of Vertebrate Animals used for Experimental and Other Scientific Purposes (CETS #123) and the Spanish legislation (R.D. 53/2013).

MPTP and melatonin treatments

Embryos at 24 hpf were used for the treatments with time course periods of 2 and 4 days. At 24 hpf, embryos were dechorionated manually and randomly distributed in 24-well plate (six embryos per well) containing treated and untreated E3 medium in a total volume of 1 mL. A stock solution of MPTP (Sigma-Aldrich, Madrid, Spain) was freshly prepared in E3 medium at a concentration of 50 mM, and was then added to the zebrafish E3 medium at a final concentration of 600 μ M. A stock solution of 200 μ M melatonin (Fagro'n Ibérica, Barcelona, Spain) was prepared in 1% dimethylsulfoxide (DMSO):E3 medium; 5 μ L of this stock was added to 1 mL of the embryo's incubation medium to obtain a final concentration of 1 μ M, corresponding to DMSO at a final concentration of 0.005%. A similar procedure was used to prepare a 40 μ M stock solution of melatonin and to obtain a final concentration of 0.2 μ M.

Embryos were exposed to MPTP from 24 to 72 hpf.

For the neuroprotective experiments, melatonin was added together with MPTP from 24 to 72 hpf. Two additional groups of zebrafish embryos were monitored up to 120 hpf. Both groups were incubated with MPTP from 24 to 72 hpf, and a 1 μ M final concentration of melatonin was added to one group from 24 to 120 hpf together with MPTP (MPTP + aMT 5 days: preventive treatment), while melatonin was added to the other group from 72 to 120 hpf (MPTP + aMT 2 days: recovery treatment). The control groups received vehicle (DMSO). Half of the solution in each group was replaced daily by a fresh prewarmed solution. After following the experimental protocols (72 and 120 hpf), the embryos were anesthetized with tricaine and then sacrificed. A schedule for this experimental method is published elsewhere.¹⁵

Gene expression analyses

Total cellular RNA from frozen embryo tissue was extracted and electrophoresed in 1.5% agarose to check for RNA integrity. RNA was extracted using the RNeasy Lipid Tissue Mini kit (Qiagen, Hilden, Germany). Total RNA was quantified by optical density at 260/280 nm and was then used to generate cDNA with the aid of a High Capacity cDNA Reverse Transcription Kit (Applied Biosystems, Foster City, CA). Amplification was performed using quantitative real-time PCR according to the standard curve method, with specific TaqMan probes (Applied Biosystems) for the targeted zebrafish genes *sod2* (Dr03100019_m1), *gpx1a* (Dr03071768_m1), and *gsr* (Dr03109438_m1), with the zebrafish *actb1* (Dr03432610_m1) probe being used as standard loading control.

Sample preparation and western blot analysis

Western blot analyses were carried out on 50 pooled 72 hpf zebrafish embryos. Samples were homogenized in buffer A (50 mM Tris-HCl, 0.15 M NaCl, 1% Triton X-100, 1 mM 1,4-dithiothreitol (DTT), pH 7.6) with a protease inhibitor cocktail (Thermo Scientific, Madrid, Spain). Homogenates were sonicated and centrifuged (5 min at 1000 g at 4°C), and the resultant supernatant was used for western blot analysis. Proteins were quantified by Bradford assay, and 40 μ g of protein was mixed with sample buffer. After denaturation (5 min at 99°C), samples were loaded onto 12% sodium dodecyl sulfate-polyacrylamide gel electrophoresis. Extracts were electrophoresed using the mini-PROTEAN Tetra Cell electrophoresis system (Biorad, Madrid, Spain). The proteins were transferred onto polyvinylidene difluoride (PVDF) membranes using a mini Trans-blot Cell (Bio-Rad) and then probed with target antibodies. Protein-antibody interactions were detected with peroxidase-conjugated horse anti-mouse or anti-rabbit immunoglobulin G antibodies using Amersham ECL Prime Western Blotting Detection Reagent (GE Healthcare Sciences, Barcelona, Spain).

Two molecular weight markers were used: Precision Plus Protein Kaleidoscope Prestained protein standards (Bio-Rad, Madrid, Spain), and Protein Marker VI (PanReac AppliChem, Panreac Quimica SLU, Barcelona, Spain). Bands were quantified using Kodak Image Station 2000R (Eastman Kodak Co., Rochester, NY) and a Kodak 1D 3.6 software. Protein bands intensity was normalized to RPL13A, and data were expressed in percent terms to control embryos. The following primary antibodies were used: anti-LC3I and LC3II (NB100-2220, Novus Biologicals, Bionova, Barcelona, Spain); anti-Mfn2 [sc-50331 (H-68); Santa Cruz Biotechnology, Quimigen, Madrid, Spain]; p62/SQSTM1 polyclonal antibody (18420-1-AP; Proteintech, AntibodyBcn, Barcelona, Spain); and anti-RPL13A (ab96074; Abcam) as a standard loading control.

Mitochondrial respiration

The oxygen consumed by an organism is produced by both non-mitochondrial and mitochondrial respiration. Non-mitochondrial oxygen consumption is derived from many sources, such as peroxisomes and plasma membrane nicotinamide adenine dinucleotide phosphate (NADPH)-oxidase activity. Mitochondrial respiration can be primarily divided into

respiration due to ATP turnover and respiration due to proton leak through the mitochondrial inner membrane to the matrix. The oxygen consumed was measured by an XFe24 Extracellular Flux Analyzer (Seahorse Bioscience, Copenhagen, Denmark). This noninvasive system facilitates the *in vivo* determination of mitochondrial bioenergetics in embryos. Respiration measurement is expressed as an oxygen consumption rate (OCR, in pmol O₂/min). One embryo was placed in each well in the XFe24 24-well islet capture plates (except for background correction wells) with 700 μ L E3 medium, and capture screens were placed over the embryos to hold them in place.¹⁴ The respiration of the zebrafish mitochondria was sequentially measured according to the following schedule: first, the basal oxygen consumption was determined; then, oligomycin was added to inhibit complex V, enabling proton leak to be determined (non-phosphorylating or resting respiration) and ATP production to be estimated; under these conditions, it was possible to calculate the fraction of basal mitochondrial respiration coupled to ATP production. Carbonyl cyanide *p*-trifluoromethoxyphenylhydrazone (FCCP), an uncoupler of oxidative phosphorylation was then added to obtain the maximal respiratory capacity or electron transfer system (ETS) capacity; lastly, antimycin A and rotenone, inhibitors of complex III and CI, respectively, were added to obtain non-mitochondrial respiration.

In the preliminary experiments, we observed that 50 min after the addition of oligomycin (100 min after initiating the experiment), a plateau was reached and then maintained. We stopped adding oligomycin after 50 min and continued to add FCCP to shorten the total period of the experiment to avoid embryo impairment.

The schedule of the inhibitor injections in the Seahorse equipment for 72 hpf zebrafish embryos was as follows: port A, 50 μ L of 150 μ M oligomycin (10 μ M final); port B, 100 μ L of 21.25 μ M FCCP (2.5 μ M final); port C, 100 μ L of 4.75 μ M FCCP (3 μ M final); and port D, 50 μ L of 200 μ M antimycin A and 200 μ M rotenone (10 μ M final). The inhibitors injections schedule for 120 hpf zebrafish embryos was as follows: port A, 50 μ L of 150 μ M oligomycin (10 μ M final); port B, 100 μ L of 34 μ M FCCP (4 μ M final); port C, 100 μ L of 4.75 μ M FCCP (4.5 μ M final); and port D, 50 μ L of 200 μ M antimycin A and 200 μ M rotenone (10 μ M final). Oxygen consumption data are expressed as pmol/min/embryo.

Redox state measurement

Glutathione peroxidase (GPx) activity was spectrophotometrically measured in homogenates of 100 pooled of 72 hpf zebrafish embryos following NADPH oxidation for 5 min at 340 nm in a Power Wave_x plate-reader spectrofluorometer (Bio-Tek Instruments, Inc., Winooski, VT), using the Glutathione Peroxidase Activity Colorimetric Assay Kit (BioVision Incorporated, Milpitas, CA). Glutathione reductase (GRd) was measured in 72 hpf embryo homogenates following the generation of 5-thio-2-nitrobenzoic acid for 10 min at 405 nm in a Power Wave_x plate-reader spectrofluorometer with the aid of the Glutathione Reductase Activity Colorimetric Assay Kit (BioVision Incorporated). Enzyme activity was expressed as nmol/min/mg prot.

Superoxide dismutase (SOD) activity was assayed with Superoxide Dismutase Activity Assay Kit (BioVision Incorporated). This activity was measured in the homogenates following the generation of water-soluble formazan dye (WST-1) using SOD from bovine erythrocytes as standard (Sigma-Aldrich, St. Louis). SOD activity was expressed as nmol/min/mg prot.

Glutathione (GSH) and oxidized glutathione (GSSG) were measured according to the slightly modified Hissig and Hilf fluorometric method.¹⁸ Briefly, 72 hpf embryo homogenates were deproteinized with 10% ice-cold trichloroacetic acid and centrifuged at 20,000 *g* for 15 min at 4°C. To measure GSH, 10 μ L supernatants were incubated with 10 μ L ethanolic *o*-phthalaldehyde solution (1 mg/mL) and 180 μ L phosphate buffer (100 mM sodium phosphate, 5 mM ethylenediaminetetraacetic acid-Na₂, pH 8.0) for 15 min at room temperature (RT). Sample fluorescence was then measured at 340 nm excitation and 420 nm emission in a FLX 800 Microplate fluorescence reader (Bio-Tek Instruments, Inc.). To measure GSSG, 30 μ L supernatants aliquots were pre-incubated with a 12 μ L *N*-ethylmaleimide solution (5 mg/mL in distilled water) for 40 min at RT, and then alkalinized

with 0.1 M NaOH. Aliquots of 45 μ L were then incubated with 10 μ L *o*-phthalaldehyde solution and 145 μ L 0.1 M NaOH for 15 min at RT. The fluorescence was then measured. GSH and GSSG concentrations were calculated according to appropriately prepared standard curves. GSH and GSSG levels are expressed as nmol/mg prot.

Determination of the melatonin, N1-acetyl-N2-formyl-5-methoxy kinuramine and N1-acetyl-5-methoxy kinuramine concentration by high resolution mass spectrometry

Melatonin, N1-acetyl-5-methoxy kinuramine (AMK) and N1-acetyl-N2-formyl-5-methoxy kinuramine (AFMK) were extracted from homogenates of 40 embryos at 72 hpf. Samples were extracted with chloroform, agitated for 10 min and centrifuged at 3800 g for 10 min, with the aqueous phase being removed by aspiration. They were then agitated for 10 min with 0.1 N NaOH and centrifuged for 10 min at 3800 g, and the aqueous phase was aspirated. Finally, the organic phase was evaporated in a Speed Vac system at a pressure of 5.1 Pa for 45 min (SPD 2010 Speed Vac System; Fisher Scientific, Madrid, Spain).

The samples were analyzed using a WATERS Acquity H Class liquid chromatograph coupled to a mass spectrometer equipped with a Waters Xevo TQ-S triple quadrupole analyzer and an Acquity UPLCr BEH C18 1.7 μ m column. Separation was performed using a gradient program at a flow rate of 0.4 mL/min (solvent A: 0.1% formic acid in water, solvent B: acetonitrile 0.1% formic acid). The set-up parameters were as follows: capillary voltage, 2.5 kV; flow rates for the gas cone and desolvation gas, 150 and 800 L/h, respectively; reference and desolvation temperatures, 150°C and 350°C, respectively.

The data were acquired using MassLynx 4.0 software and calibrated and quantified with the aid of the QuanLynx package.

Mortality and malformation

The mortality rate was calculated as the percentage of dead embryos with respect to total embryos. Edema, the most common malformations, along with tail and yolk abnormalities were macroscopically quantified.

Statistical analysis

Statistical analyses were carried out using the GraphPad Prism 6 software (GraphPad; Software, Inc., La Jolla, CA). Data are expressed as the mean \pm standard error of the mean of 3–15 independent experiments per group. One-way analysis of variance and the *post hoc* Tukey test were used to compare differences between the experimental groups. A *p* value of 0.05 was considered to be statistically significant.

Results

Melatonin protects mitochondria against bioenergetic failure caused by MPTP in 72 hpf embryos

The significant reduction in mitochondrial CI activity caused by the administration of 600 μ M MPTP at 72 hpf in a similar experimental model reported elsewhere¹⁵ was expected to result in mitochondrial bioenergetic deficiency.

In vivo measurement of O₂ consumption in the 72 hpf embryos treated with MPTP showed a sharp decline in respiration function, as evidenced by a reduction in basal respiration and ETS capacity after the addition of FCCP (Fig. 1A, B) as compared to untreated embryos (*p* < 0.001). MPTP also increased proton leak and, consequently, the L/E (LEAK respiration/ETS capacity) coupling control ratio, reflecting a significant impairment of the mitochondrial inner membrane (MIM) (*p* < 0.001, Fig. 1C, D). As expected, these changes led to a sharp reduction in ATP turnover (*p* < 0.001, Fig. 1E). A representative sequence of *in vivo* respiratory events is shown in Figure 1F.

The addition of melatonin to zebrafish embryos dose-dependently mitigated mitochondrial bioenergetic impairment induced by MPTP by restoring ETS capacity and MIM integrity

(Fig. 1B, D). Consequently, zebrafish mitochondria were able to rescue ATP turnover ($p < 0.001$, Fig. 1E), MPTP treatment increased the mortality rate and malformations in the zebrafish larvae at 72 and 120 hpf (Fig. 2A–D; arrows denote malformations in Fig. 2E). Treatment of 72 and 120 hpf embryos with MPTP increased the mortality rate up to 10% ($p < 0.05$) and 14% ($p < 0.01$), respectively (Fig. 2A, C). The main malformations produced by MPTP were abnormal yolk differentiation and tail curvature ($p < 0.05$), with only a slight increase in edema (Fig. 2B, D, and Supplementary Tables S1 and S2; Supplementary Data are available online at www.liebertpub.com/zeb). Melatonin treatment rescued this phenotype and lowered the mortality rate to that of the control group ($p < 0.05$, Fig. 2A–D, and Supplementary Tables S1 and S2).

To assess whether the effects of melatonin depend on its presence in the embryo and/or its metabolism, the levels of the indoleamines, AFMK, and AMK, were measured in the medium and zebrafish homogenates. The results show the presence of small amounts of melatonin, AFMK and AMK in untreated and MPTP-treated embryos. After the addition of melatonin to the medium, its content in embryos increased significantly both in the presence and absence of MPTP depending on the dose ($p < 0.001$, Fig. 3A, B). Although AFMK was not detected in the medium, it increased in the embryos, while AMK was detected in both the medium and embryos. In both cases, melatonin metabolites levels were much lower than those of melatonin (Fig. 3C–E).

On the whole, these results suggest that melatonin plays a protective role not only against MPTP-induced mitochondrial dysfunction induced by CI inhibition but also against its phenotypic consequences. The neuroprotective properties of AFMK and AMK reported elsewhere can be ruled out in this case due to the low level of these catabolites.¹⁹

Melatonin protects embryos against oxidative damage induced by MPTP in 72 hpf embryos

The inhibition of CI activity typically results in enhanced electron leak and reactive oxygen species (ROS) formation, which further damage the mitochondria and limit their ATP production capacity. We next analyzed oxidative stress status and antioxidant responses to these conditions.

The GSSG/GSH ratio, which accurately reflects the intracellular redox status,²⁰ increased significantly in embryos incubated with MPTP ($p < 0.001$, Fig. 4A). This finding suggests that the embryo shifts to a hyperoxidative status; this depends on excess GSSG production ($p < 0.001$, Fig. 4B), which is not properly converted into GSH ($p < 0.001$, Fig. 4C). The GSH redox cycle depends on the activity of two enzymes, GPx and GRd, acting in tandem. GPx activity involves the oxidation of two GSH molecules into one GSSG molecule, which was expected to be NADPH-dependently reduced to GSH by GRd. The decline in GPx activity and, particularly, in GRd activity ($p < 0.001$, Fig. 4D, E) explains the accumulation of GSSG during MPTP treatment (Fig. 4B). The primary cause of the disruption in the GSH cycle by MPTP is probably the failure of SOD-dependent first-line antioxidant defenses. Indeed, the sharp reduction in SOD activity in embryos incubated with MPTP ($p < 0.001$, Fig. 4F) produces an oxidative status capable of damaging enzymes in the next line of antioxidant defenses (GPx and particularly GRd). The mRNA expression of both *sod* and *gpx* also decreased significantly (Fig. 4G, I), which helps to explain the embryo's reduced capacity to protect against MPTP-induced ROS formation. However, an increase in *grd* mRNA expression was observed under these conditions ($p < 0.001$, Fig. 4H), thus suggesting the presence of a different type of regulatory mechanism that offsets the sharp decline in this enzyme's activity, which is highly sensitive to damage caused by ROS.

The presence of melatonin in the embryo incubation medium counteracted the prooxidative response to MPTP, which normalized the GSSG/GSH ratio ($p < 0.001$, Fig. 4A) and, thus, restored intracellular redox equilibrium. This can be explained by melatonin's ability to restore antioxidant enzymes activity and expression reported elsewhere (Fig. 4D–I),^{21,22} which, in turn, normalizes the GSH cycle required to control redox status.

Melatonin enhances autophagy and reduced mitochondrial fusion induced by MPTP in 72 hpf embryos

Melatonin was previously found to be involved in regulating autophagy. We then attempted to determine whether the rescue of zebrafish by melatonin is associated with increased autophagic flux. We therefore analyzed the content of autophagosomal component LC3 as an autophagic marker. Here, the levels of LC3-I and LC3-II were significantly reduced by MPTP treatments as compared to control group ($p < 0.001$ and $p < 0.05$, respectively; Fig. 5A, B). In addition, embryos treated with MPTP showed a significant increase in the mitofusin (Mfn2) level ($p < 0.001$, Fig. 5C). Melatonin treatment blunted the effect of MPTP on LC3 levels, with LC3-I levels being restored by both doses of melatonin ($p < 0.001$ for MPTP + aMT 1 μ M and $p < 0.01$ for MPTP + aMT 0.2 μ M, Fig. 5A), and LC3-II levels by 1 μ M of melatonin ($p < 0.01$, Fig. 5B).

We concluded the autophagy study by analyzing the autophagic flow marker p62. Our results show that significantly increased p62 levels MPTP ($p < 0.001$, Fig. 5D). Both melatonin doses counteracted the effect of MPTP and restored the levels of p62 ($p < 0.001$, Fig. 5D), a finding that correlates with the changes observed in LC3I and LC3II. Finally, the embryos treated with 1 μ M melatonin showed a significant decrease in Mfn2 as compared to the group treated with MPTP ($p < 0.01$, Fig. 5C).

Melatonin prevents and repairs mitochondrial failure induced by MPTP in 120-hpf embryos

To determine whether the neuroprotective properties of melatonin described in this study not only prevent the effects of MPTP on zebrafish embryos but also rescue these embryos once the parkinsonian phenotype is established, we used a different experimental paradigm. The zebrafish embryos were incubated with MPTP from 24 to 72 hpf and were then maintained up to 120 hpf in the absence of MPTP to assess whether the neurodegenerative process persisted. A second group of embryos was incubated with 1 μ M melatonin from 24 to 120 hpf during a 5-day preventive treatment period, while a third group of embryos was treated with 1 μ M melatonin from 72 to 120 hpf during a 2-day recovery treatment period.

We analyzed *in vivo* O₂ consumption in the 120 hpf embryos treated with MPTP both with and without the administration of melatonin. Respiratory function declined sharply in the MPTP-treated embryos, which is in line with the 80% decrease in CI activity noted elsewhere.¹⁵ We observed a decrease in both basal respiration ($p < 0.001$) and ETS capacity ($p < 0.01$) as compared to the control group (Fig. 6A, B). MPTP caused an increase in proton leak ($p < 0.05$, Fig. 6C) as compared to the control group and also in the L/E coupling control ratio ($p < 0.001$, Fig. 6D), which corresponded to significant mitochondrial inner membrane impairment in the 72 hpf embryos. These changes led to a sharp reduction in ATP turnover in the MPTP-treated embryos as compared to controls ($p < 0.05$, Fig. 6E). The addition of melatonin to the medium during MPTP preventive treatment time (MPTP + aMT5) and after the removal of MPTP from the medium (MPTP + aMT2, recovery therapy) protected the mitochondria from bioenergetic failure induced by MPTP, which restored basal respiration ($p < 0.001$) and ETS capacity ($p < 0.05$) (Fig. 6A, B). Proton leak decreased significantly in the melatonin-treated embryos as compared to those treated with MPTP and control groups ($p < 0.001$, Fig. 6C). Consequently, both melatonin treatments significantly reduced the L/E coupling control ratio as compared to the MPTP-treated group ($p < 0.001$, Fig. 6D) and were able to restore ATP turnover ($p < 0.001$, Fig. 6E). A representative sequence of the *in vivo* respiratory events is shown in Figure 6F.

Melatonin prevents and restores the expression of antioxidant enzymes inhibited by MPTP in 120 hpf embryos

Treatment with MPTP significantly reduced *gpx* and *sod* mRNA expression in 120 hpf embryos

compared to the control group ($p < 0.001$, Fig. 7A, B), which is similar to that recorded for 72 hpf embryos. Treatment with melatonin (+aMT5) counteracted the effect of MPTP on *gpx* and *sod* mRNA expression ($p < 0.001$, Fig. 7A, B) and raised *grd* mRNA expression above that of the control group ($p < 0.05$, Fig. 7C). On the other hand, melatonin did not modify the effects of MPTP when administered only after the removal of MPTP (+aMT2) (Fig. 7A–C).

Discussion

In this study, we used a parkinsonian zebrafish model described elsewhere²³ to monitor *in vivo* mitochondrial bioenergetic changes between 72 and 120 hpf. Neurodegeneration and mitochondrial impairment were found to occur in zebrafish embryos when treated with MPTP from 24 to 72 hpf. Interestingly, these pathophysiological events were found to persist and even to worsen in the absence of MPTP from 72 to 120 hpf. This model also enabled us to evaluate the protective role of melatonin in relation to mitochondrial impairment, thus demonstrating for the first time that it not only prevents MPTP-induced bioenergetic failure but also restores normal mitochondrial function. These observations are also applicable to oxidative stress following mitochondrial damage. Melatonin counteracted the reduction in autophagy and the increase in mitochondrial fusion induced by MPTP.

In addition, it is important to note that the XFe24 Extra-cellular Flux Analyzer (Seahorse Bioscience, Billerica, MA) enabled us to analyze mitochondrial function in the intact animal even at 120 hpf. Consequently, the data collected using this method, which enable all mitochondria, both healthy and damaged to be analyzed, more accurately reflect the embryo's bioenergetic state.

We used CI inhibition as a starting point for studying the mechanisms underlying mitochondrial impairment in PD.^{1,2} With the aid of MPTP, a neurotoxin that specifically inhibits CI and blocks dopamine uptake by dopaminergic cells,⁶ we previously showed that zebrafish embryos developed the principal features of PD: neuroinflammation, tyrosine hydroxylase, dopaminergic neurons loss, and significantly reduced motility.¹⁵

These effects, which were already detected at 72 hpf, persisted after 48 h of MPTP treatment and worsened after an additional 48 h in the absence of MPTP up to 120 hpf. We show that 600 nM MPTP causes a significant reduction in basal respiratory capacity and ETS, and an increase in the L/E ratio, which reflect reduced oxygen consumption and mitochondrial inner membrane damage, respectively. Consequently, mitochondrial bioenergetic capacity after administration of MPTP was reduced, leading to a decrease in ATP turnover (Fig. 6A–E). These changes are closely in line with the inhibition of the *parkin/PINK1/DJ-1* network expression by MPTP at 72 hpf reported elsewhere, leading to the accumulation of damaged mitochondria.^{15,23,24}

Interestingly, at 120 hpf, that is, 48 h after the removal of MPTP from the embryos, the inhibition of *parkin/PINK1/DJ-1* expression further worsened, thus demonstrating that the neurodegenerative process persists in absence of MPTP.¹⁵ These findings suggest a parallel deterioration in mitochondrial conditions. To assess this hypothesis, we carried out a prior analysis of CI activity in untreated 120 hpf embryos, which was four-fold higher than at 72 hpf.¹⁵

We also found that basal respiration and ETS levels were higher in untreated embryos at 120 hpf than at 72 hpf, with a lower L/E ratio also being recorded (Figs. 1B and 6B). Altogether, these data reflect an improvement in mitochondrial capacity over the period development. Basal respiration and ETS remained low, while the L/E ratio increased after the removal of MPTP, which is in line with the inhibition of CI reported under similar experimental conditions.¹⁵ Overall, both mitochondria and ATP tended to be slightly less affected at 120 hpf than at 72 hpf. These data suggest that the selective inhibition of CI activity by MPTP reduces mitochondrial respiratory capacity and ATP turnover, which are typical features in both genetic and neurotoxic-induced models of PD.^{11,25}

Mitochondrial dysfunction following CI inhibition increases reactive oxygen species (ROS) formation, which, in turn, oxidizes mtDNA and other electron transport chain (ETC) components, and contributes to bioenergetic impairment.²⁶ ROS may subsequently affect other mitochondria-related proteins such as Pink1, Parkin, and DJ-1,²⁷ which are involved in cel-

lular protection against oxidative damage.^{5,28–30} Inactivation of these proteins inhibits the autophagy/mitophagy pathways required to remove damaged mitochondria.^{24,31} Given the inhibition of the mRNA expression and Pink1, Parkin, and DJ-1 protein content reported elsewhere,¹⁵ we assessed the presence of oxidative stress in our experimental model.

Treatment with MPTP significantly inhibited SOD and GPx activity and expression, which is consistent with an enhanced GSSG/GSH ratio in 72-hpf embryos (Fig. 4). The activity of GRd, the other enzyme in the GSH cycle, which is highly sensitive to oxidative damage,³² also decrease after treatment with MPTP, but was not offset by enhanced the GRd mRNA expression. Analysis of the antioxidative enzymes at 120 hpf 48 h after the removal of MPTP showed that GPx and SOD expression remained inhibited with no induction of GRd expression (Fig. 7). The absence of normal antioxidant defense together with the persistence CI inhibition, even in absence of MPTP, produce mitochondrial failure and continued ROS formation, maintain neurodegenerative processes in the brain of zebrafish embryos.^{15,33,34}

Mitochondria are subject to a high degree of dynamic processes including fission, fusion and mitophagy. Changes in fission and fusion plasticity depend on cellular energy demands,³⁵ while mitophagy is activated to remove excessively damaged mitochondria, thus preventing mitochondrial oxidative stress.³⁶ To gain a more in-depth picture of mitochondrial fate in our experimental model, we analyzed LC3, p62, and Mfn2 expression in embryos at 72 hpf. We found that MPTP reduced LC3-I and LC3-II expression and increased p62 and Mfn2 expression (Fig. 5). These results are consistent with a reduction in autophagic mechanisms, which favors the accumulation of damaged mitochondria in the brain of zebrafish embryos.

In addition, we observed a reduction in the global bioenergetic capacity of the dopaminergic system mitochondria, which increases oxidative damage. Moreover, when bound to Parkin, Mfn2 induces mitochondrial fusion through PINK1-dependent phosphorylation.^{37,38} Our data showed enhanced *Mfn2* expression, but it cannot be phosphorylated by PINK1 due to the significant MPTP-related reduction in both parkin and PINK1.¹⁵ It remains unclear whether enhanced *Mfn2* expression is associated with an attempt to compensate for its inactivation. However, it is possible to suggest that the reduction in LC3-I and LCR-II expression, increase in p62 expression, and probable absence of *Mfn2* activation alter mitochondrial dynamics, which typically occurs in neurodegenerative disorders such as PD.³⁵

After deciphering the mitochondrial changes underlying neurodegeneration in zebrafish embryos, we attempted to determine whether melatonin, an indoleamine with known neuroprotective properties, can also prevent mitochondrial dysfunction and/or restore mitochondrial normalcy. In a first set of experiments, melatonin was highly effective in dose-dependently preventing mitochondrial damage induced by MPTP, with 1 μ M of melatonin found to be normally more effective than 0.2 μ M. Melatonin also prevented oxidative stress by maintaining antioxidative enzyme expression and activity and the GSSG/GSH ratio (Fig. 4).

In a second set of experiments, melatonin was effective in both preventive and recovery treatments, returning mitochondria to their normal bioenergetic capacity. These findings show, for the first time, that melatonin possesses curative properties through its ability to normalize deficient mitochondria in the model of parkinsonism here reported.

These well-known beneficial effects of melatonin depend on two different sets of mechanisms: (1) enhancement of CI activity, reduction of mitochondrial oxygen consumption, improved bioenergetic efficiency and increased ATP production,^{20,21,39–41} and (2) reduced oxidative stress through direct ROS scavenging and indirect enhancement of antioxidant enzyme expression and activity.^{8,22,42} After scavenging ROS, melatonin is converted into two principal metabolites, AFMK and AMK, which have antioxidant and neuroprotective properties.^{19,43} However, their low levels here showed indicate that these metabolites are not very involved in the protective mechanisms of melatonin (Fig. 3).

Moreover, the capacity of melatonin to normalize LC3-I, LC3-II, and p62 expression and to reduce *Mfn2* expression (Fig. 5), points to the activation of a novel mechanism, which regulates autophagic events and mitochondrial dynamics.⁴⁴ In addition to recently published data on the restoration of the parkin/PINK1/DJ-1/MUL1 network by melatonin a similar experimental model,¹⁵ our study provides a more in-depth insight into the molecular

pathways involved in melatonin protection against parkinsonian neurodegeneration.

Finally, this study provides fresh evidence with respect to the clinical utility and neuroprotective properties of melatonin, which, over a 2-day treatment period, restored mitochondrial dysfunction. In addition, our findings show that targeting mitochondria is undoubtedly of considerable therapeutic value in the treatment of Parkinson's disease.⁴⁵

Acknowledgments

This study was partially supported by grants from the Ministerio de Economía, Industria y Competitividad and from the Fondo de Desarrollo Regional Feder Spain nº CB/10/ 00238; from the Consejería de Innovación, Ciencia y Empresa, Junta de Andalucía (P07-CTS-03135 and P10-CTS-5784). M.E.D.-C. is a PhD student supported by the Consejería de Innovación, Ciencia y Empleo, Junta de Andalucía, Spain; M.F.-O. and A.H.-G. have a FPU scholarship from the Ministerio de Educación, Cultura y Deporte, Spain; and L.C.L. is supported by the "Ramón y Cajal" National Program (Ministerio de Economía y Competitividad, Spain). Finally, we wish to thank Michael O'Shea for proofreading the article.

Disclosure Statement

No competing financial interests exist.

References

1. Franco-Iborra S, Vila M, Perier C. The Parkinson disease mitochondrial hypothesis: where are we at? *Neuroscientist* 2015;22:266–277.
2. Schapira AH, Cooper JM, Dexter D, *et al.* Mitochondrial complex I deficiency in Parkinson's disease. *J Neurochem* 1990;54:823–827.
3. Li L, Tan J, Miao Y, Lei P, Zhang Q. ROS and autophagy: interactions and molecular regulatory mechanisms. *Cell Mol Neurobiol* 2015;35:615–621.
4. Von SS, Nardin A, Schrepfer E, Ziviani E. Mitochondrial dynamics and mitophagy in Parkinson's disease: a fly point of view. *Neurobiol Dis* 2015;90:58–67.
5. Abou-Sleiman PM, Muqit MM, Wood NW. Expanding insights of mitochondrial dysfunction in Parkinson's disease. *Nat Rev Neurosci* 2006;7:207–219.
6. Przedborski S, Jackson-Lewis V, Yokoyama R, *et al.* Role of neuronal nitric oxide in 1-methyl-4-phenyl-1,2,3,6-tetrahydropyridine (MPTP)-induced dopaminergic neurotoxicity. *Proc Natl Acad Sci U S A* 1996;93:4565–4571.
7. Acuña-Castroviejo D, Escames G, Venegas C, *et al.* Extra-pineal melatonin: sources, regulation, and potential functions. *Cell Mol Life Sci* 2014;71:2997–3025.
8. Acuña-Castroviejo D, Lopez LC, Escames G, *et al.* Melatonin-mitochondria interplay in health and disease. *Curr Top Med Chem* 2011;11:221–240.
9. Reiter RJ, Tan DX, Mayo JC, *et al.* Melatonin as an antioxidant: biochemical mechanisms and pathophysiological implications in humans. *Acta Biochim Pol* 2003;50:1129–1146.
10. Falkenburger BH, Saridaki T, Dinter E. Cellular models for Parkinson's disease. *J Neurochem* 2016;139:121–130.
11. Jagmag SA, Tripathi N, Shukla SD, Maiti S, Khurana S. Evaluation of models of Parkinson's disease. *Front Neurosci* 2015;9:503.
12. Doerrier C, Garcia JA, Volt H, *et al.* Permeabilized myocardial fibers as model to detect mitochondrial dysfunction during sepsis and melatonin effects without disruption of mitochondrial network. *Mitochondrion* 2016;27:56–63.
13. Gibert Y, McGee SL, Ward AC. Metabolic profile analysis of zebrafish embryos. *J Vis Exp* 2013;e4300.
14. Stackley KD, Beeson CC, Rahn JJ, Chan SS. Bioenergetic profiling of zebrafish embryonic development. *PLoS One* 2011;6:e25652.

15. Diaz-Casado ME, Lima E, Garcia JA, *et al.* Melatonin rescues zebrafish embryos from the parkinsonian phenotype restoring the parkin/PINK1/DJ-1/MUL1 network. *J Pineal Res* 2016;61:96–107.
16. Lima-Cabello E, Diaz-Casado ME, Guerrero JA, *et al.* A review of the melatonin functions in zebrafish physiology. *J Pineal Res* 2014;57:1–9.
17. Westerfield M. *The Zebrafish Book. A Guide for the Laboratory Use of Zebrafish (Danio rerio)*. Univ Oregon Press, Eugene, OR, 2007.
18. Hissin PJ, Hilf R. A fluorometric method for determination of oxidized and reduced glutathione in tissues. *Anal Biochem* 1976;74:214–226.
19. Leon J, Escames G, Rodriguez MI, *et al.* Inhibition of neuronal nitric oxide synthase activity by N1-acetyl-5-methoxykynuramine, a brain metabolite of melatonin. *J Neurochem* 2006;98:2023–2033.
20. Martin M, Macias M, Escames G, Leon J, Acuna-Castroviejo D. Melatonin but not vitamins C and E maintains glutathione homeostasis in t-butyl hydroperoxide-induced mitochondrial oxidative stress. *FASEB J* 2000;14:1677–1679.
21. Acuna-Castroviejo D, Escames G, Rodriguez MI, Lopez LC. Melatonin role in the mitochondrial function. *Front Biosci* 2007;12:947–963.
22. Garcia JA, Volt H, Venegas C, *et al.* Disruption of the NF- κ B/NLRP3 connection by melatonin requires retinoid-related orphan receptor- α and blocks the septic response in mice. *FASEB J* 2015;29:3863–3875.
23. Kitada T, Tong Y, Gautier CA, Shen J. Absence of nigral degeneration in aged parkin/DJ-1/PINK1 triple knockout mice. *J Neurochem* 2009;111:696–702.
24. Pickrell AM, Youle RJ. The roles of PINK1, parkin, and mitochondrial fidelity in Parkinson's disease. *Neuron* 2015; 85:257–273.
25. Trancikova A, Tsika E, Moore DJ. Mitochondrial dysfunction in genetic animal models of Parkinson's disease. *Antioxid Redox Signal* 2012;16:896–919.
26. Murphy MP. How mitochondria produce reactive oxygen species. *Biochem J* 2009;417:1–13.
27. Requejo-Aguilar R, Bolanos JP. Mitochondrial control of cell bioenergetics in Parkinson's disease. *Free Radic Biol Med* 2016;100:123–137.
28. Canet-Aviles RM, Wilson MA, Miller DW, *et al.* The Parkinson's disease protein DJ-1 is neuroprotective due to cysteine-sulfinic acid-driven mitochondrial localization. *Proc Natl Acad Sci U S A* 2004;101:9103–9108.
29. Kuroda Y, Mitsui T, Kunishige M, *et al.* Parkin enhances mitochondrial biogenesis in proliferating cells. *Hum Mol Genet* 2006;15:883–895.
30. Wood-Kaczmar A, Gandhi S, Yao Z, *et al.* PINK1 is necessary for long term survival and mitochondrial function in human dopaminergic neurons. *PLoS One* 2008;3:e2455.
31. van der Merwe C, Jalali Sefid DZ, Christoffels A, Loos B, Bardiën S. Evidence for a common biological pathway linking three Parkinson's disease-causing genes: parkin, PINK1 and DJ-1. *Eur J Neurosci* 2015;41:1113–1125.
32. Huang J, Philbert MA. Cellular responses of cultured cerebellar astrocytes to ethacrynic acid-induced perturbation of subcellular glutathione homeostasis. *Brain Res* 1996; 711:184–192.
33. Hang L, Thundiyil J, Lim KL. Mitochondrial dysfunction and Parkinson disease: a Parkin-AMPK alliance in neuroprotection. *Ann N Y Acad Sci* 2015;1350:37–47.
34. Schapira AH. Etiology of Parkinson's disease. *Neurology* 2006;66:S10–S23.
35. Burte F, Carelli V, Chinnery PF, Yu-Wai-Man P. Disturbed mitochondrial dynamics and neurodegenerative disorders. *Nat Rev Neurol* 2015;11:11–24.
36. Lee J, Giordano S, Zhang J. Autophagy, mitochondria and oxidative stress: cross-talk and redox signalling. *Biochem J* 2012;441:523–540.
37. Chen Y, Dorn GW. PINK1-phosphorylated mitofusin 2 is a Parkin receptor for culling damaged mitochondria. *Science* 2013;340:471–475.
38. Vives-Bauza C, Przedborski S. Mitophagy: the latest problem for Parkinson's disease. *Trends Mol Med* 2011;17: 158–165.
39. Khaldy H, Escames G, Leon J, Bikjdaouene L, Acuna-Castroviejo D. Synergistic

- effects of melatonin and de- prenyl against MPTP-induced mitochondrial damage and DA depletion. *Neurobiol Aging* 2003;24:491–500.
40. Lopez A, Garcia JA, Escames G, *et al.* Melatonin protects the mitochondria from oxidative damage reducing oxygen consumption, membrane potential, and superoxide anion production. *J Pineal Res* 2009;46:188–198.
 41. Martin M, Macias M, Escames G, *et al.* Melatonin-induced increased activity of the respiratory chain complexes I and IV can prevent mitochondrial damage induced by ruthenium red in vivo. *J Pineal Res* 2000;28:242–248.
 42. Tan DX, Manchester LC, Esteban-Zubero E, Zhou Z, Reiter RJ. Melatonin as a potent and inducible endogenous antioxidant: synthesis and metabolism. *Molecules* 2015;20:18886–18906.
 43. Galano A, Tan DX, Reiter RJ. On the free radical scavenging activities of melatonin's metabolites, AFMK and AMK. *J Pineal Res* 2013;54:245–257.
 44. Lin C, Chao H, Li Z, *et al.* Melatonin attenuates traumatic brain injury-induced inflammation: a possible role for mitophagy. *J Pineal Res* 2016;61:177–186.
 45. Schapira AH, Patel S. Targeting mitochondria for neuroprotection in Parkinson disease. *JAMA Neurol* 2014;71: 537–538.

Figure 1

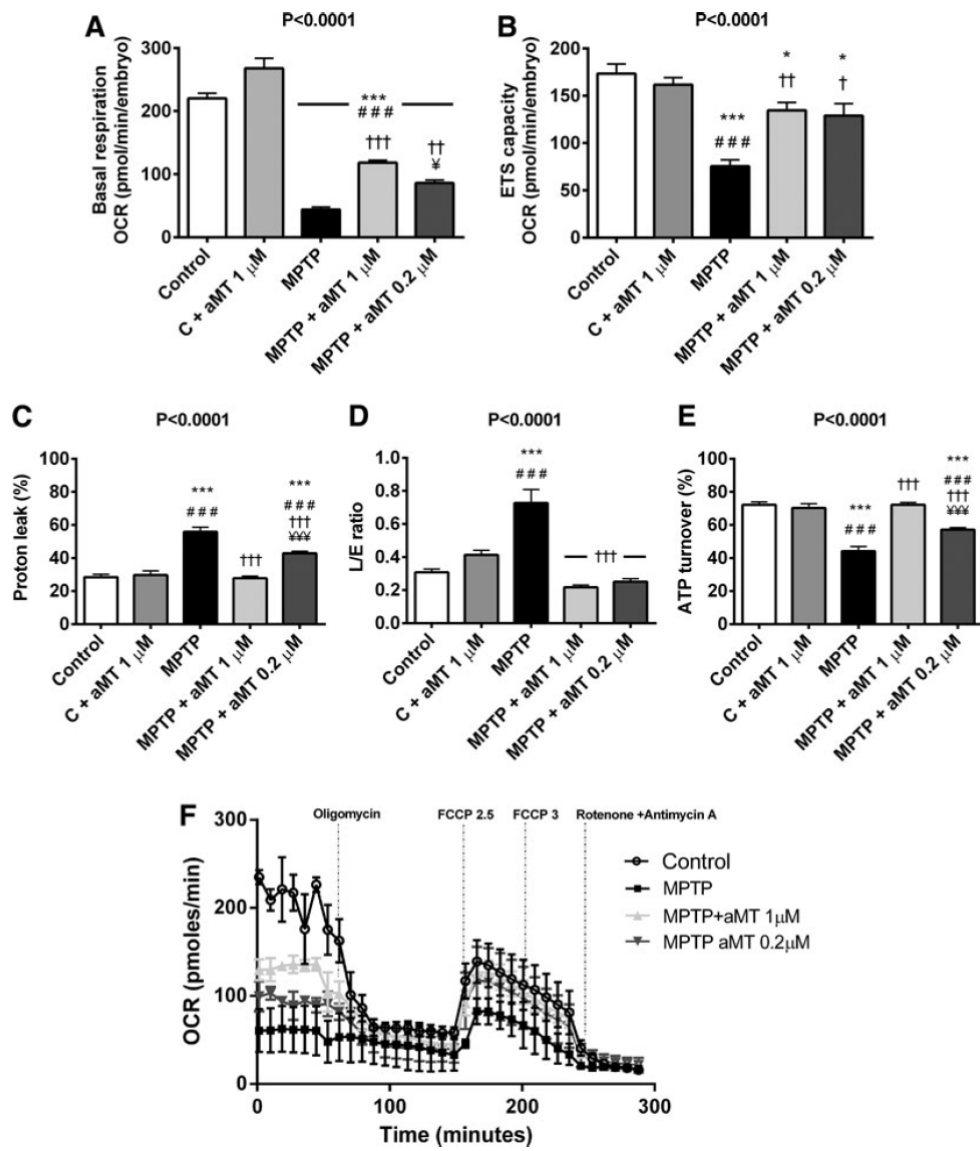


Figure 2

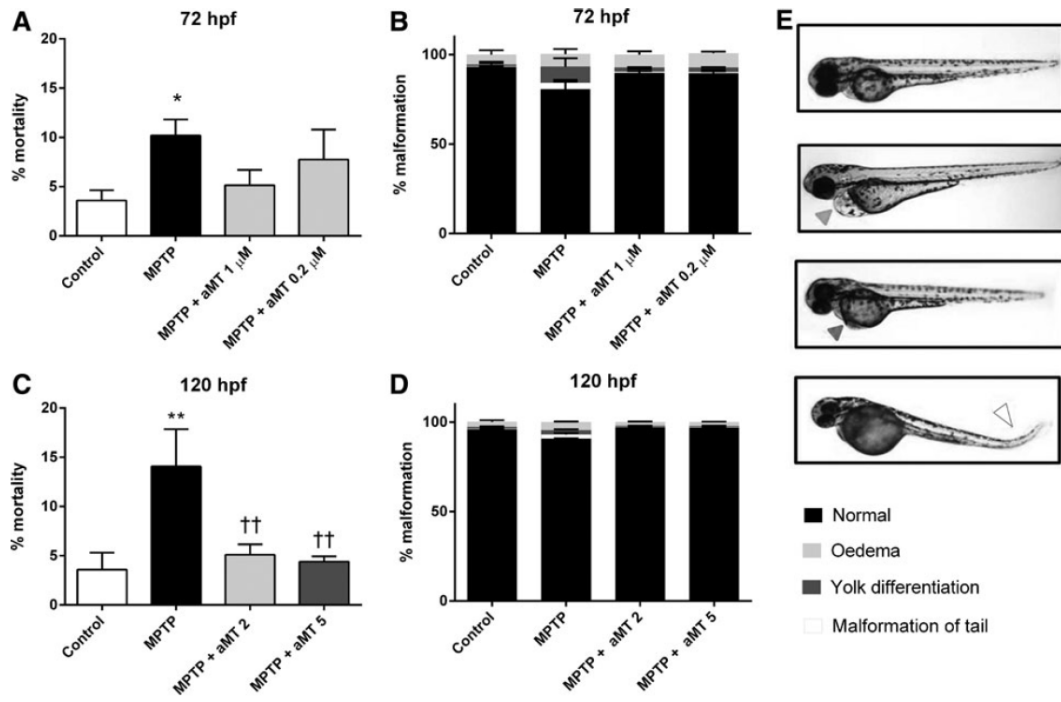


Figure 3

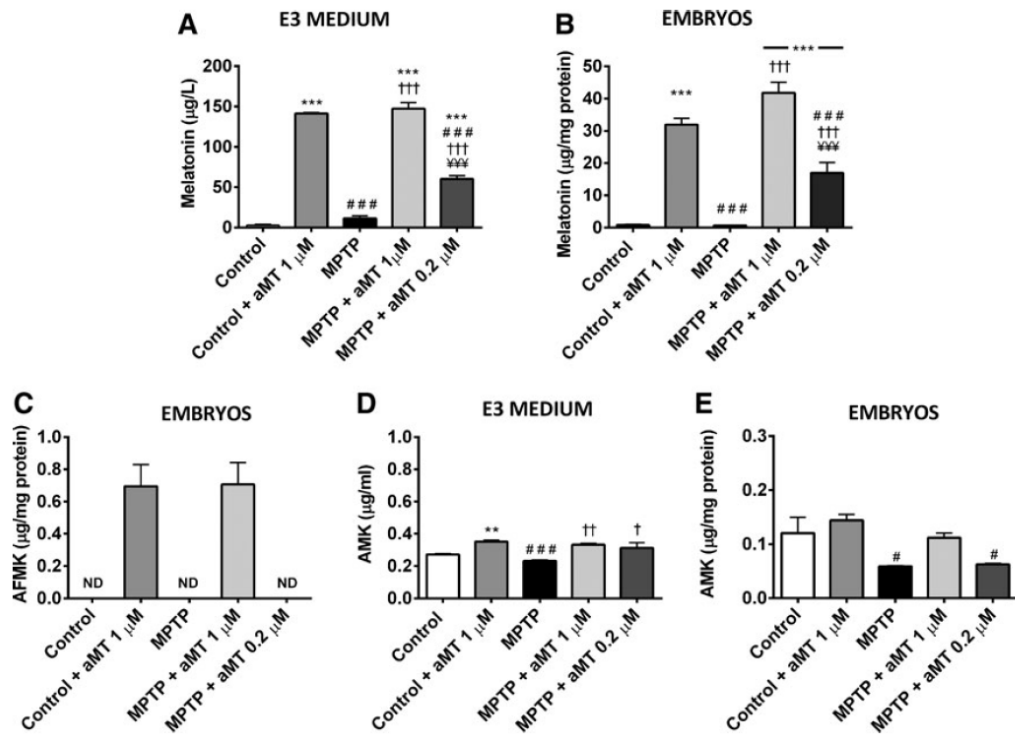


Figure 4

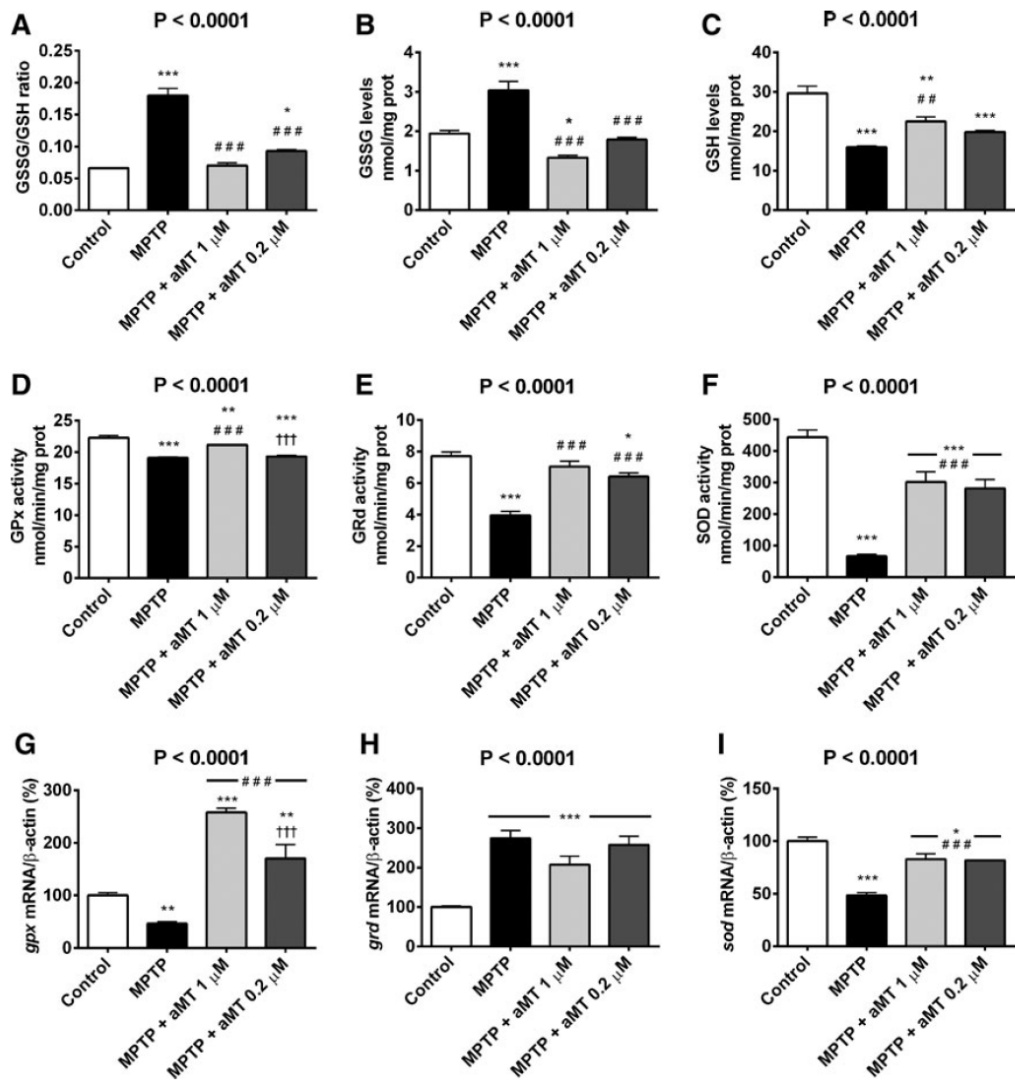


Figure 5

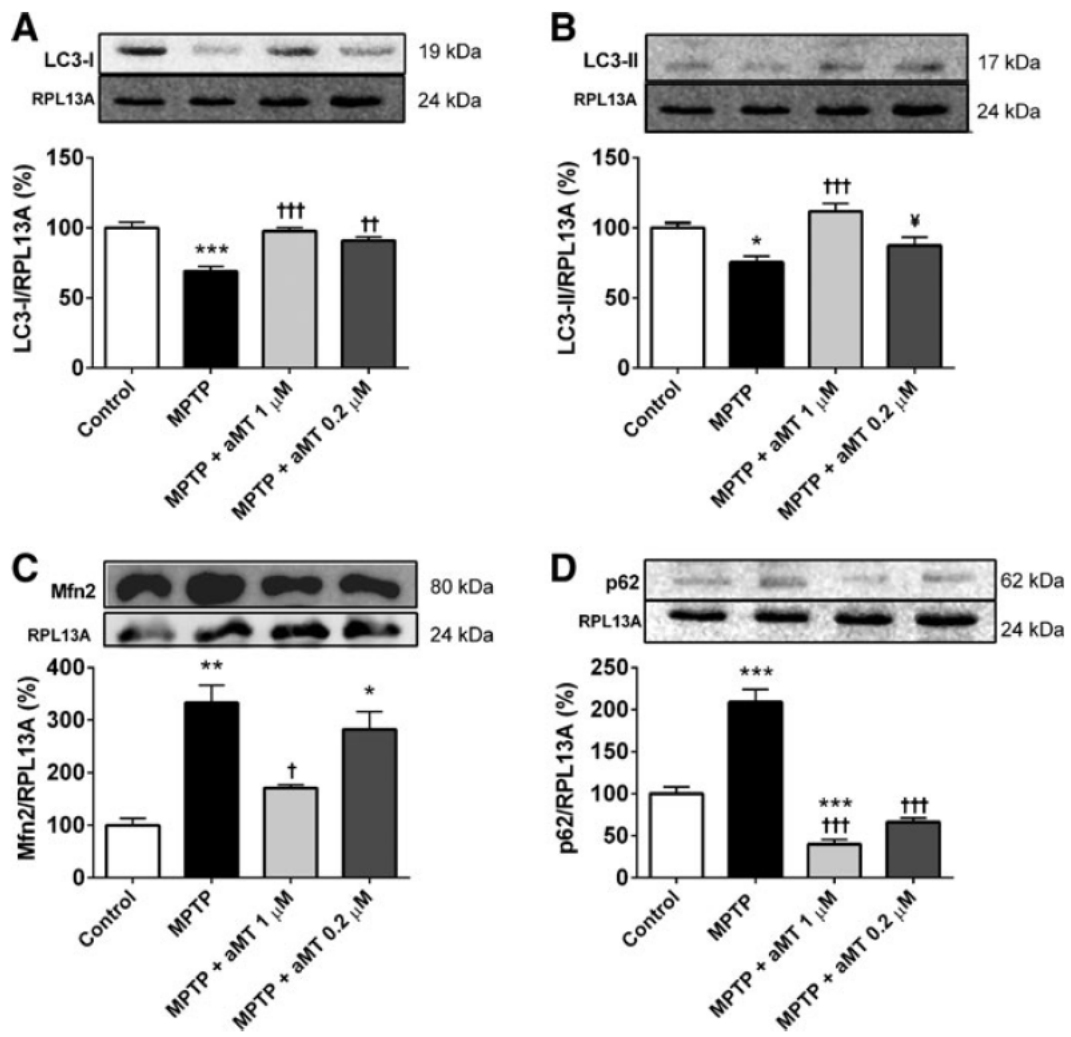


FIG. 1. Melatonin prevented mitochondrial impairment due to MPTP. Embryos were treated with MPTP and aMT at 24 hpf and mitochondrial respiration was analyzed *in vivo* 48 h later, at 72 hpf. (A) Basal respiration. (B) ETS capacity. (C) Percentage of proton leak. (D) L/E (proton leak/ETS) ratio. (E) ATP turnover. Melatonin restored mitochondrial bioenergetics at lower doses (0.2 IM). In all cases, melatonin had no effect when added to zebrafish embryos in the absence of MPTP. Melatonin treatment in control embryos had no effect. (F) Representative recordings of OCR obtained from respiratory analysis in zebrafish embryos. Data are presented as mean – SEM. * $p < 0.05$, and *** $p < 0.001$ versus control; ### $p < 0.001$ versus control + aMT 1 IM; † $p < 0.05$, †† $p < 0.01$, and ††† $p < 0.001$ versus MPTP; †††† $p < 0.05$ and ††††† $p < 0.001$ versus aMT 1 IM. One-way ANOVA with Tukey's *post hoc* test ($n = 10–15$ embryos). MPTP, 1-methyl-4-phenyl-1,2,3,6-tetrahydropyridine; aMT, melatonin (*N*-acetyl-5-methoxytryptamine); ETS, electron transfer system; OCR, oxygen consumption rate; hpf, hours postfertilization; SEM, standard error of the mean; ANOVA, analysis of variance.

FIG. 2. Mortality and macroscopic malformation rates observed in zebrafish embryos subjected to different treatments. (A) Mortality in 72 hpf embryos; (B) Malformation rate in 72 hpf embryos. Treatment with MPTP induced an increase of malformations, which were reduced by the administration of melatonin. (C) Mortality rate in 120 hpf embryos. (D) Malformation rate in 120 hpf embryos. Embryos treated with MPTP showed a higher malformation rate than control and embryos treated with melatonin. (E) Embryos imaged at 72 hpf showing each of the malformations analyzed. Arrows mark the malformation in the embryo: curvature in the tail, edema and alterations in the yolk. Data are expressed as described in Figure 1. Data are presented as mean – SEM. * $p < 0.05$, ** $p < 0.01$ versus control; †† $p < 0.01$ versus MPTP. One-way ANOVA with Tukey's *post hoc* test ($n = 500$ embryos).

FIG. 3. Melatonin, AMK, and AFMK concentration. (A) Melatonin concentration in E3 medium. (B) Melatonin concentration in 72 hpf embryos. (C) AFMK concentration in 72 hpf embryos. (D) AMK concentration in E3 medium. (E) AMK concentration in 72 hpf embryos. Data expressed as described in Figure 1. ** $p < 0.01$ and *** $p < 0.001$ versus control; † $p < 0.05$ and ### $p < 0.001$ versus control + aMT; † $p < 0.05$, †† $p < 0.01$ and ††† $p < 0.001$ versus MPTP; †††† $p < 0.001$ versus aMT 1 IM. One-way ANOVA with Tukey's *post hoc* test ($n = 5$). AFMK, *N*1-acetyl-*N*2-formyl-5-methoxykynuramine; AMK, *N*1-acetyl-5-methoxykynuramine; ND, no detected.

FIG. 4. Melatonin prevented a hyperoxidative state occurring after mitochondrial impairment induced by MPTP. Embryos were treated with MPTP and melatonin at 24 hpf and analyzed 48 h later at 72 hpf. (A) GSSG/GSH ratio. (B) GSSG levels. (C) GSH levels. (D–F) Enzyme activity in GSH cycle. (D) GPx activity; (E) GRd activity; (F) SOD activity. (G–I) Changes in enzyme mRNA expression in the glutathione cycle. (G) mRNA expression levels of *gpx*. (H) mRNA expression levels of *grd*. (I) mRNA expression levels of *sod*. In all cases, administration of melatonin restored these parameters to normal values, even at doses of 0.2 IM. Data expressed as described in Figure 1. * $p < 0.05$, ** $p < 0.01$, and *** $p < 0.001$ versus control; †† $p < 0.01$, and ††† $p < 0.001$ versus MPTP; †††† $p < 0.001$ versus aMT 1 IM. One-way ANOVA with Tukey's *post hoc* test ($n = 5–8$). GPx, glutathione peroxidase; GRd, glutathione reductase; GSH, reduced glutathione; GSSG, glutathione disulfide; SOD, superoxide dismutase.

FIG. 5. Melatonin prevents the effects of MPTP on autophagy and mitochondrial fusion in 72 hpf embryos. (A) LC3-I levels. Melatonin blunts MPTP effect on LC3-I content. (B) LC3-II levels. MPTP treatment decreased LC3-II levels, while 1 IM melatonin counteracted this effect. (C) Levels mitofusin (Mfn2). Mfn2 content was increased by MPTP treatment while melatonin decreased Mfn2 levels. (D) p62 levels. Melatonin normalizes p62 levels. Data expressed as described in Figure 1. * $p < 0.05$, ** $p < 0.01$, and *** $p < 0.001$ versus control; † $p < 0.05$, †† $p < 0.01$ and ††† $p < 0.001$ versus MPTP; †††† $p < 0.05$ versus aMT 1 IM. One-way ANOVA with Tukey's *post hoc* test ($n = 3$).

Acknowledgments

This study was partially supported by grants from the Ministerio de Economía, Industria y Competitividad and from the Fondo de Desarrollo Regional Feder Spain n° CB/10/00238; from the Consejería de Innovación, Ciencia y Empresa, Junta de Andalucía (P07-CTS-03135 and P10-CTS-5784). M.E.D.-C. is a PhD student supported by the Consejería de Innovación, Ciencia y Empleo, Junta de Andalucía, Spain; M.F.-O. and A.H.-G. have a FPU scholarship from the Ministerio de Educación, Cultura y Deporte, Spain; and L.C.L. is supported by the “Ramón y Cajal” National Program (Ministerio de Economía y Competitividad, Spain).

Finally, we wish to thank Michael O'Shea for proofreading the article.

